Molecular Therapy
Oncolytics
Original Article

Reolysin and Histone Deacetylase Inhibition in the Treatment of Head and Neck Squamous Cell Carcinoma

Alena C. Jaime-Ramirez,[1] Jun-Ge Yu,[2] Enrico Caserta,[3] Ji Young Yoo,[1] Jianying Zhang,[4] Tae Jin Lee,[5] Craig Hofmeister,[3] John H. Lee,[6] Bhavna Kumar,[2] Quintin Pan,[2] Pawan Kumar,[2] Robert Baiocchi,[3] Theodoros Teknos,[2] Flavia Pichiorri,[3] Balveen Kaur,[1] and Matthew Old[2]

[1]Department of Neurological Surgery, The Ohio State University, Columbus, OH 43210, USA; [2]Department of Otolaryngology-Head and Neck Surgery, The James Cancer Hospital and Solove Research Institute, The Ohio State University, Columbus, OH 43210, USA; [3]Department of Internal Medicine, The Ohio State University, Columbus, OH 43210, USA; [4]Biomedical Informatics Department, Center for Biostatistics, Wexner Medical Center, The Ohio State University, Columbus, OH 43210, USA; [5]Department of Molecular Virology, Immunology, and Medical Genetics, The Ohio State University, Columbus, OH 43210, USA; [6]Department of Otolaryngology/Head and Neck Surgery, Sanford Health, Sioux Falls, SD 57105, USA

Oncolytic viruses (OVs) are emerging as powerful anti-cancer agents and are currently being tested for their safety and efficacy in patients. Reovirus (Reolysin), a naturally occurring non-pathogenic, double-stranded RNA virus, has natural oncolytic activity and is being tested in phase I–III clinical trials in a variety of tumor types. With its recent US Food and Drug Administration (FDA) orphan drug designation for several tumor types, Reolysin is a potential therapeutic agent for various cancers, including head and neck squamous cell carcinomas (HNSCCs), which have a 5-year survival of ~55%. Histone deacetylase inhibitors (HDACis) comprise a structurally diverse class of compounds with targeted anti-cancer effects. The first FDA-approved HDACi, vorinostat (suberoylanilide hydroxamic acid [SAHA]), is currently being tested in patients with head and neck cancer. Recent findings indicate that HDAC inhibition in myeloma cells results in the upregulation of the Reolysin entry receptor, junctional adhesion molecule 1 (JAM-1), facilitating reovirus infection and tumor cell killing both in vitro and in vivo. In this study, we tested the anti-tumor efficacy of HDAC inhibitors AR-42 or SAHA in conjunction with Reolysin in HNSCCs. While HDAC inhibition increased JAM-1 and reovirus entry, the impact of this combination therapy was tested on the development of anti-tumor immune responses.

INTRODUCTION

Oncolytic viruses (OVs) are emerging as potentially powerful anti-cancer agents; talimogene laherparepvec (T-VEC) was approved for treatment of unresectable metastatic melanoma, and numerous trials are currently testing the safety and efficacy of a variety of OVs in patients.[1,2] Reovirus is a naturally occurring non-pathogenic, double-stranded RNA virus that was isolated from human respiratory and gastrointestinal tracts and has been extensively studied in a similar fashion to T-VEC.[3] Reolysin is a type 3 Dearing reovirus (Oncolytics Biotech) and is currently being tested in phase I–III clinical trials in a variety of tumor types.[3] With its recent orphan drug designation from the US Food and Drug Administration (FDA) for ovarian, gastric, peritoneal, pancreatic, and brain cancers, Reolysin is a potential therapeutic agent for several types of cancer, including head and neck squamous cell carcinomas (HNSCCs). Despite aggressive treatments, the diagnosis of locally advanced head and neck cancer carries a dismal prognosis, with fewer than 55% of patients predicted to survive longer than 5 years.[4] Thus, there is a clear need for novel therapies with activity against these tumors.

Histone deacetylase inhibitors (HDACis) comprise a structurally diverse class of compounds that are targeted anti-cancer agents.[5] The first FDA-approved HDACi, vorinostat (suberoylanilide hydroxamic acid [SAHA]), is highly effective in the treatment of cutaneous T cell lymphoma.[6] Similar to Reolysin, SAHA is also being investigated for safety and efficacy in patients with head and neck cancer and preliminary results are promising.[7] HDAC inhibition in myeloma cells has recently been reported to upregulate the Reolysin entry receptor, junctional adhesion molecule 1 (JAM-1), and allows for greater Reolysin infection and killing both in vitro and in vivo in myeloma-bearing nude mice.[8] Importantly, the prevalence of JAM-1 in various cancer types has yet to be thoroughly explored. Moreover, the effect of HDAC inhibition on JAM-1 in HNSCCs and its immunological impact in immune-competent mice remains to be elucidated.

Since HDAC inhibition is a promising approach for head and neck cancers, we tested the impact of HNSCC tumor cell treatment with

Received 4 January 2017; accepted 3 May 2017;
http://dx.doi.org/10.1016/j.omto.2017.05.002.

Correspondence: Matthew Old, MD, Department of Otolaryngology-Head and Neck Surgery, The Ohio State University, Starling Loving Hall, Room B217, 320 W. 10th Avenue, Columbus, OH 43210, USA.
E-mail: matthew.old@osumc.edu

the HDAC inhibitors AR-42 or SAHA on Reolysin entry and tumor cell killing. Using both immune-deficient and immune-competent mice, we explored the effects of this therapeutic strategy on tumor/host interactions and anti-tumor immune responses. With growing evidence of the significance of immune-mediated mechanisms in oncolytic viral therapy, we sought to characterize the impact of combining Reolysin and HDACis in the treatment of HNSCCs in an immune-competent model. Here, we observed that HDAC inhibition resulted in the significant enhancement of Reolysin replication and anti-tumor efficacy in vitro and in vivo, with enhanced immune-mediated anti-tumor responses.

RESULTS

HDAC Inhibition Increases the Susceptibility of Head and Neck Cancer Cells to Reovirus Entry

A previous study found a marked upregulation of the reovirus entry receptor, JAM-1, after treatment of myeloma cells with HDAC inhibitors.[8] To evaluate the effect of HDAC inhibition on reovirus susceptibility of patients with head and neck cancer, we tested the impact of treating SCC74A (human) and mouse tonsil epithelial (MTE) (murine) squamous carcinoma cells with HDAC inhibitors (AR-42 or SAHA) on the reovirus entry receptor (JAM-1). Flow cytometry of treated cells revealed a significant increase in JAM-1 cell surface expression after treatment with AR-42 or SAHA ($p < 0.001$) (Figure 1A). Reduced JAM-1 expression on the cell surface after reovirus infection and HDAC inhibitor treatment is consistent with receptor internalization after binding to reovirus, as indicated by western blot (WB) analysis for the reovirus capsid protein (σ-NS) (Figure S1). These data indicate that JAM-1 is upregulated after HDACi treatment and that Reolysin results in receptor internalization in head and neck cancer cells.

HDACi Enhances Reolysin Replication

Consistent with the increased cell surface receptor, HDACi treatment markedly enhanced reovirus capsid protein (σ-NS) after infection, suggesting an increase in viral entry or progeny (Figures 1A and S1). We therefore examined the effects of combinatorial treatment on Reolysin viral replication. An increase in the levels of reovirus capsid protein (represented by green fluorescence) was also observed in red fluorescent protein (RFP)-expressing SCC-74A cells treated with either AR-42 or SAHA (Figure 1B). Quantification of virus titers revealed a significant increase in viral replication (as measured in plaque-forming units [PFUs] in cells treated with AR-42 or SAHA; $p < 0.0001$) versus Reolysin treatment alone (Figure 1C). Collectively, these results indicate that HDAC inhibition of head and neck squamous carcinoma cells resulted in increased reovirus entry and replication.

HDACi and Reolysin Treatment Results in Synergistic Killing and Enhanced Inflammatory Responses

Next, we determined the impact of combinatorial therapy on human and murine head and neck squamous cancer cell killing. In the SCC-2 and SCC-74A human cancer cell lines, there was a significant and synergistic increase in tumor cell killing following HDACi plus Reolysin combination treatment, when compared to individual treatment groups ($p \leq 0.003$ in all cell lines tested) (Figures S1B, S1C, and 2A). The combination enhancement of head and neck tumor cell killing was also observed in a wide panel of cell lines (SCC-1, Cal27, SCC-11, and SCC-47) (Figures S1B and S1C). Cell viability was measured at 48 hr after treatment with HDAC inhibitors (AR-42 or SAHA) and Reolysin with concentrations at 0.0625, 0.125. 0.25, 0.5, 1, 2, and 4 times their respective IC_{50} values as described.[9] There was a synergistic interaction between AR-42 or SAHA when combined with Reolysin, indicative of a combination index (CI) value of less than one as determined by a Chou-Talalay analysis in both the SCC-2 and SCC-74A cell lines (Figure 2A). Consistent with increased virus replication, human SCC74A tumor cells treated with the combination of Reolysin and HDACis displayed significantly more dead cells, as measured by flow cytometric analysis for Annexin and propidium iodide (PI) dual-positive cells, when compared to each treatment alone ($p < 0.001$) (Figure 2B). Moreover, a significant increase in overall cell killing (Figure 2C) and apoptotic cell death (Figure S2A) was also observed in the MTE murine squamous carcinoma cell line treated with the combination of HDAC inhibitors and Reolysin versus each individual treatment group alone ($p \leq 0.01$). Taken together, these findings illustrate the ability of HDACis to synergistically interact with Reolysin and enhance HNSCC killing in vitro.

HDAC inhibition has also been shown to inhibit anti-viral immunity by blocking the cell-intrinsic type I interferon (IFN) responses.[10–12] It is also known that reovirus individual therapy induces a robust immune response, with inflammatory cytokine production and the activation of both innate and adaptive immune responses in various tumor types.[13–19] To further elucidate the role of HDACi and Reolysin combinatorial therapy on tumor cells, the pro-inflammatory cytokine expression of IFN-α and MCP-1 was assessed as previously described[20] following 24 hr of treatment in both the SCC74A and MTE cell lines. There was enhanced IFN-α expression in both the SCC74A and MTE cancer cell lines following combination treatment when compared with monotherapies. Interestingly, we observed a significant enhancement of MCP-1 expression following combination HDACi and Reolysin therapy when compared to each individual treatment group (Figure S2B) ($p < 0.05$). Collectively, these data indicate that HDACi plus Reolysin combination therapy results in a pro-inflammatory tumor cell response.

In Vivo Combinatorial Treatment Enhances Anti-tumor Efficacy and Survival

Based on in vitro findings, two murine tumor models were employed to assess the combinatorial efficacy of Reolysin and SAHA in vivo. In humans, HNSCC recurs both locally and at distant sites. Reolysin is a versatile oncolytic agent, as it can be used both intravenously or intratumorally, depending on the clinical scenario. It has been tested in clinical trials in both formats, with evidence of local effects for systemic therapy and systemic effects for local therapy.[21–24] We chose intratumoral injections for our in vivo models to mirror the clinical scenario of recurrent locoregional disease that is best treated with intratumoral injections in the clinic. This is one of the most common scenarios for many HNSCC recurrences.

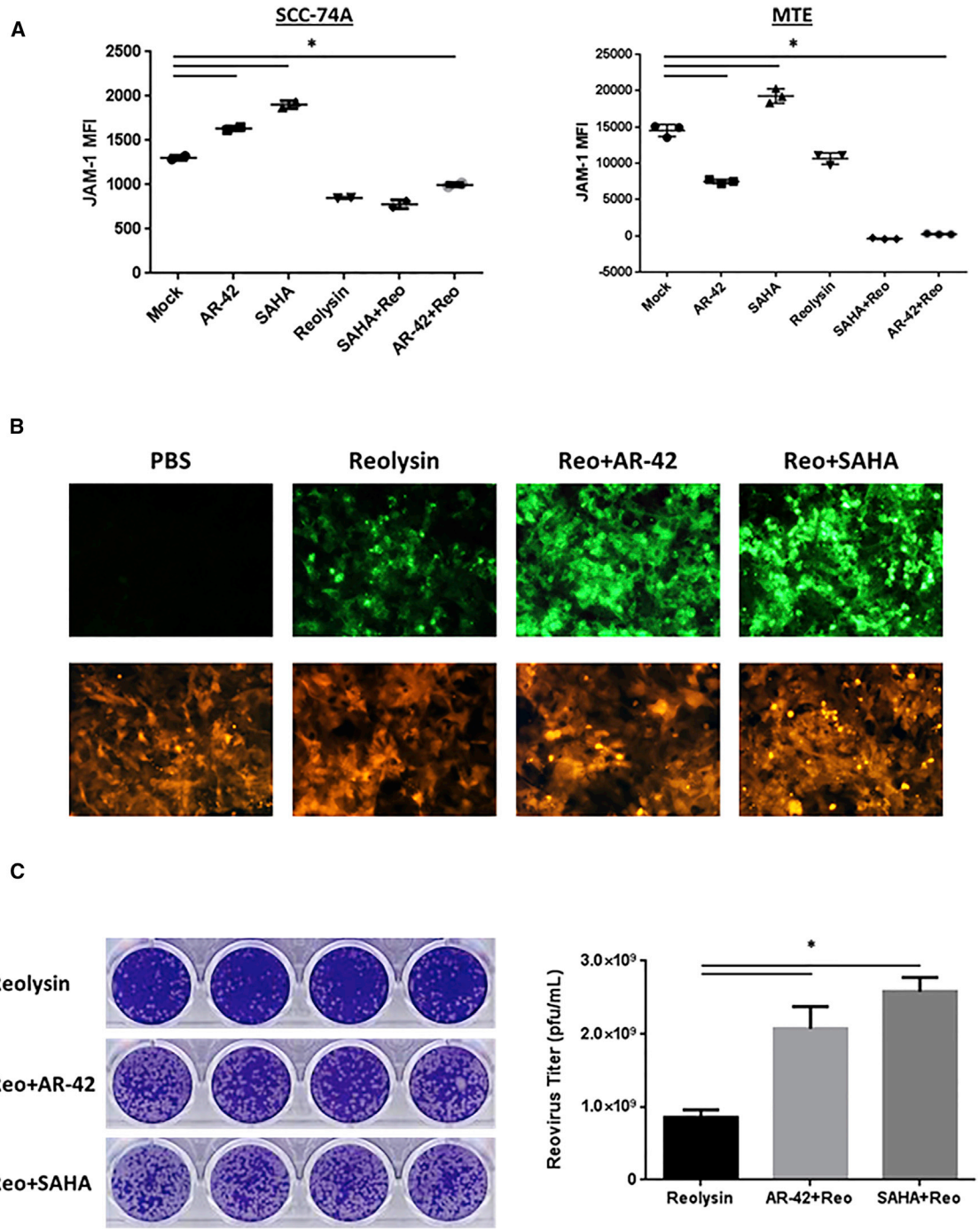

Figure 1. HDAC Inhibition Increased JAM-1 Levels and Enhanced Reolysin Replication

The expression of the reovirus entry receptor JAM-1 and Reolysin (Reo) replication was assessed following administration of AR-42 (10 μM) or SAHA (20 μM) followed by Reolysin (10 MOI) for the indicated time point on SCC74-A (human) or MTE (murine) squamous carcinoma cell lines. (A) Flow cytometric analysis of SCC74-A (left) and MTE (right) JAM-1 cell surface expression following AR-42 or SAHA and/or Reolysin for 48 hr. Data shown are the mean fluorescence intensity (MFI) of cells, with $n \geq 2$ per group ± SD. (B) Human red fluorescent protein (RFP)-expressing SCC74-A cells were assayed for the Reolysin capsid protein (green) following Reolysin plus AR-42 or SAHA treatment for 48 hr followed by immunohistochemistry. (C) SCC-74A cells were treated with Reolysin plus AR-42 or SAHA and supernatants were analyzed for reovirus replication using L929 cells using crystal violet staining in a standard plaque-forming unit (PFU) assay after 7 days. Representative images (left) of clear plaques obtained and quantification (right) of reovirus titers. *$p < 0.001$ (differences of combination-treated cells versus all other treatment groups). Data are representative of at least three independent experiments.

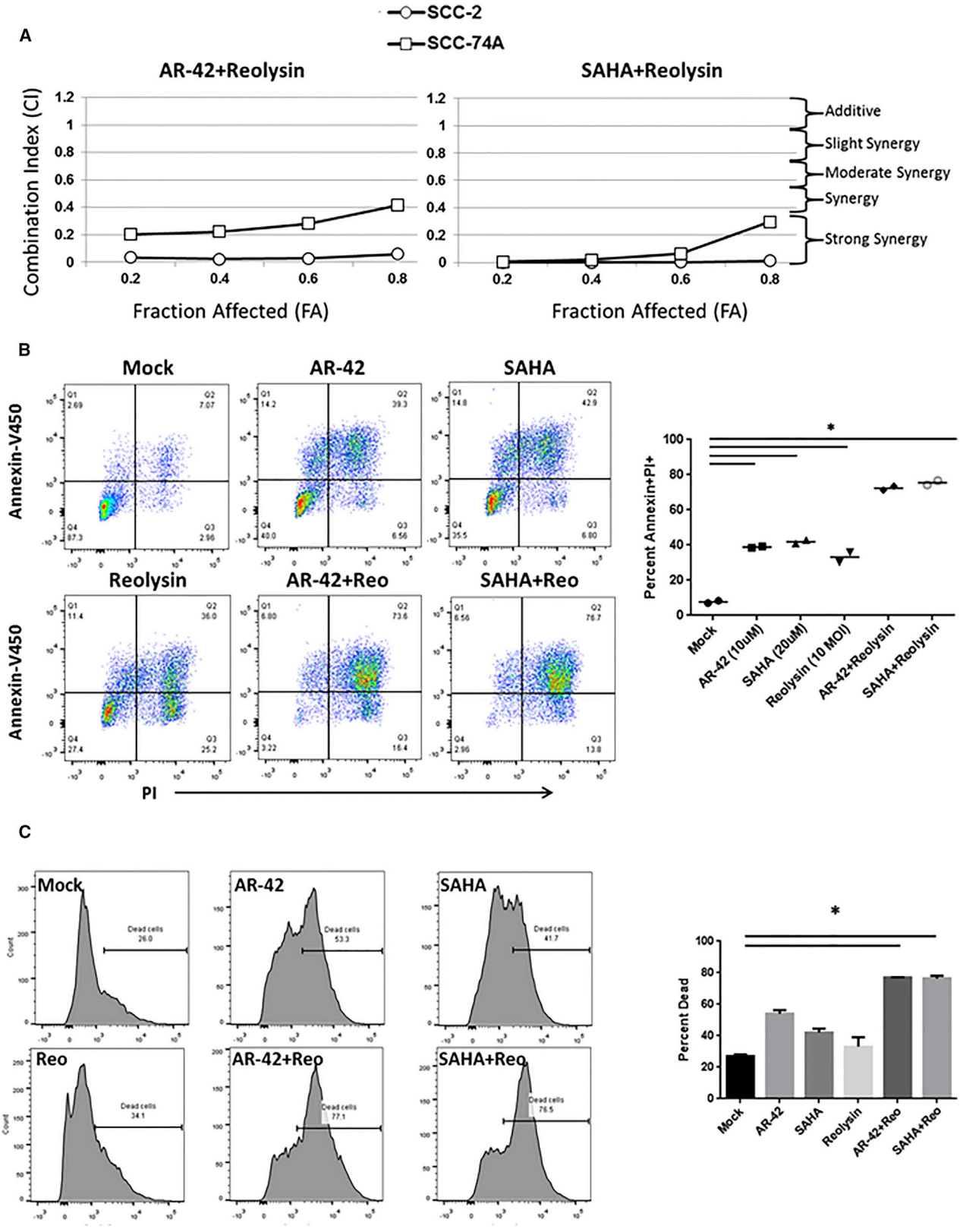

(legend on next page)

To determine the direct anti-tumoral effects of treatment, female athymic nude mice bearing human HNSCC SCC74A xenografts were treated with DMSO, SAHA, Reolysin, or combination therapy. There was a significant reduction in the rate of tumor growth in combination-treated mice versus all other treatment groups (Figure 3A, left panel) ($p < 0.01$). Kaplan-Meir survival curves of mice treated with the SAHA plus Reolysin combination displayed a significant survival advantage over mice that received the individual treatment ($p < 0.001$) (Figure 3A, right panel). Immunohistochemical (IHC) H&E analysis of tumor sections at the time of euthanasia (when tumors reached ~1,500 mm^3 after the indicated treatment) revealed an obvious immune cell infiltrate in tumors from mice treated with both SAHA and Reolysin (Figure 3B, top panels). Further characterization of these immune cells revealed a robust macrophage ($CD68^+$) infiltrate (Figure 3B, bottom panels), as well as enhanced natural killer (NK) cell presence (natural cytotoxicity triggering receptor $[NCR1]^+$) (Figure S3A, top panels).

To assess the effects of combinatorial treatment on the immune response, immune-competent wild-type mice bearing MTE syngeneic squamous tumors were utilized. Mice treated with the SAHA plus Reolysin combination had a significantly slower tumor growth rate over time ($p < 0.0001$) (Figure 4A, left panel) and a significant enhancement in murine survival when compared to each individual treatment ($p \leq 0.01$) (Figure 4A, right panel). To assess immune cell responses against the tumor, IHC analysis was performed. As with the SCC74A tumor model, a robust macrophage ($CD68^+$) response was observed (Figure 4B, top panels), with an enhanced NK cell (NCR^+) and CD4 T cell presence (Figure S3A, middle and bottom panels) in MTE tumors following HDACi plus Reolysin treatment. Interestingly, we also observed a marked increase in CD8 T cells following combinatorial therapy (Figure 4B, bottom panels).

To assess MTE-specific immune responses, total splenocytes were harvested from three mice per group at 7 days after study recruitment and co-cultured ex vivo with MTE tumor cells. Splenocytes from mice treated with SAHA plus Reolysin exhibited significantly greater MTE tumor cell-killing capacity compared to each individual treatment group, as determined by live and dead flow cytometric analysis ($p < 0.001$) (Figure 4B). Phenotypic analysis of these splenoctyes did not reveal any differences in the immune cell subsets assessed, which included activated NK cells ($CD49b^+CD335^+$), myeloid-derived suppressor cells ($CD11b^+Gr1^+$), macrophages ($CD11b^+F4/80^+$), $CD4^+$ T cells, $CD8^+$ T cells, effector $CD4^+$ or $CD8^+$ T cells ($CD4^+$ or $CD8^+$ and $CD3^+CD44^+CD62L^+$), or dendritic cells ($CD11c^+$ and $CD80^+$ or $MHCII^+$) (Figure S3B). Data obtained from both immunodeficient and immunocompetent mice suggest that HDAC inhibition improved virus entry and also augmented anti-tumor immune responses in vivo.

DISCUSSION

Treatment of head and neck cancers with HDAC inhibitors and Reolysin separately is currently being tested in patients.[7] Understanding how the mechanisms of each therapeutic, or the combination thereof, can affect tumors and the anti-tumor immune response is critical to enhancing patient outcomes. Recent reports show that HDAC inhibition in myeloma cells results in the upregulation of the Reolysin entry receptor, JAM-1, thus allowing for greater Reolysin infection and killing both in vitro and in vivo.[8] Consistent with these findings, we observed JAM-1 expression and sensitivity to Reolysin killing in HNSCC tumor cells following treatment with the HDAC inhibitors AR-42 or SAHA. Using both immune-deficient and immune-competent mice, as well as male and female mice, we explored the effects of this therapeutic strategy on the tumor as well as the anti-tumor immune response. HDAC inhibition resulted in a significant upregulation of the JAM-1 reovirus surface receptor on HNSCC cells. Moreover, this inhibition resulted in the significant enhancement of Reolysin replication and both in vitro and in vivo anti-tumor efficacy with enhanced anti-tumor immune responses.

In accordance with the epigenetic regulation of JAM-1 and its induction following treatment with HDAC inhibition in multiple myeloma,[8] we also observed JAM-1 receptor upregulation and increases in reovirus replication in HNSCCs. The synergistic killing activity and pro-inflammatory responses following HDAC inhibition in combination with Reolysin highlight the therapeutic potential of combination therapy with the induction of potentially immunogenic[25] cell death in both human and murine cell lines. While apoptotic cell death is often dysregulated in cancer cells,[26,27] combination therapy resulted in a robust and significant increase in tumor cell apoptosis.

Although HDACi-induced cell death can be highly immunogenic,[28,29] HDAC inhibition has been shown to inhibit anti-viral immunity via blocking both cell-intrinsic type 1 IFN responses as well as NK cell function.[10–12,30] HDAC inhibition is also thought to have a

Figure 2. HDACi and Reolysin Combination Treatment Results in Synergistic Killing via Apoptosis Induction

The impact of HDACi (AR-42 or SAHA) and Reolysin (Reo) combinatorial therapy was assessed on human (SCC-2 and SCC-74-A) and murine (MTE) squamous carcinoma cell killing and apoptosis. (A) Human head and neck cancer cell lines were treated with 0.0625, 0.125. 0.25, 0.5, 1, 2, and 4 times the IC_{50} concentration of each HDACi and/or Reolysin for 48 hr followed by a standard MTT assay. A Chou-Talalay analysis of combinatorial killing percentages is indicated with the fraction affected (FA) versus combination index (CI) plots. CI < 1 indicates synergy, CI = 1 indicates additive, and CI > 1 indicates antagonistic combination interactions. (B) Representative propidium iodide (PI) and Annexin-V450 scatterplots and quantification of SCC-74A head and neck cancer cells treated with PBS, AR-42, SAHA, Reolysin or the combination of each HDACi plus Reolysin for 48 hr. The right panel shows the quantification of apoptosis for SCC-74A-treated cells as indicated (n = 2/group). (C) MTE murine squamous carcinoma cells were treated with AR-42 (10 μM) or SAHA (20 μM) and/or 10 MOI of Reolysin for 48 hr. Tumor cell killing was then assessed via live and dead cell staining. Representative live/dead cell histograms from flow cytometric analysis and quantification of dead cells. *$p \leq 0.01$ (combination treatment differences compared to each individual treatment group). All experiments were performed in triplicate.

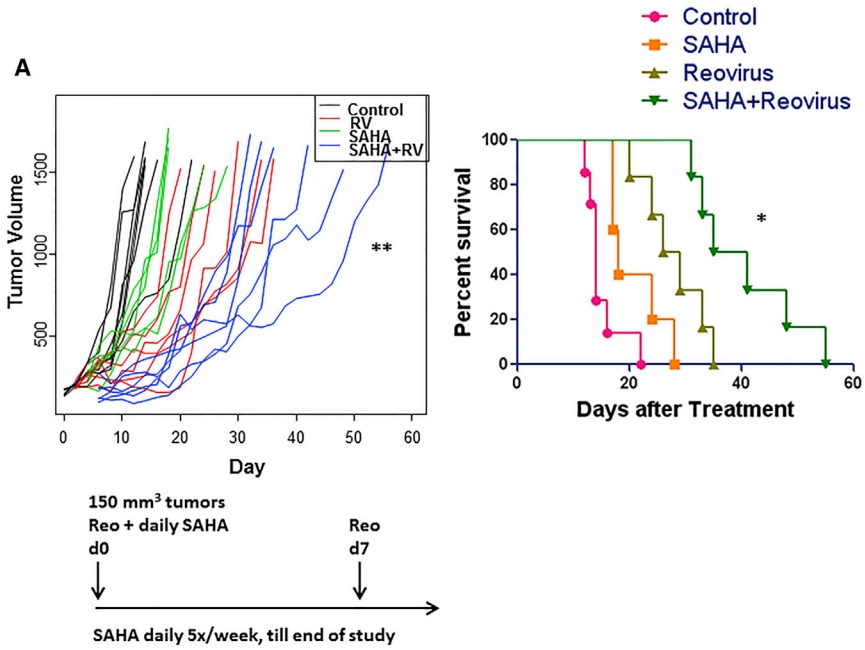

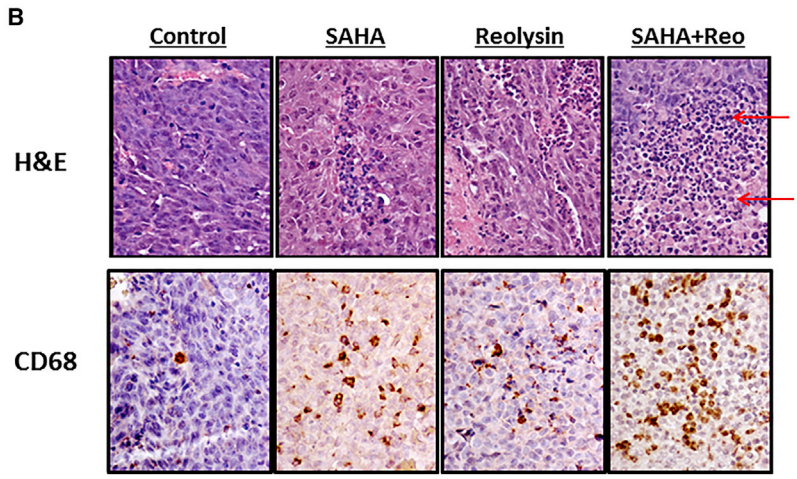

Figure 3. In Vivo Efficacy of SAHA and Reolysin Is Enhanced in a Human Xenograft Model of Head and Neck Cancer

Nude athymic female mice (n = 10 per group) bearing subcutaneous SCC-74A human xenograft tumors (treatment started at 150 mm^3) were treated with DMSO, SAHA (50 mg/kg), Reolysin (Reo) (2×10^8 PFU), or SAHA plus Reolysin combinatorial therapy. (A) Tumor volume growth was assessed over time for each mouse in every treatment group. **$p < 0.01$ (difference between combination-treated mice and all other treatment groups; left panel). Kaplan-Meir survival curves for mice bearing subcutaneous SCC-74A tumors treated with SAHA, reovirus (RV), or the indicated combination (the treatment schema is provided below the plot). *$p \leq 0.001$ (combination treatment differences compared to each individual treatment group; right panel). All survival studies were performed in duplicate. (B) Representative H&E- and macrophage (CD68)-stained tumors at time of death when tumors reached ~1,500 mm^3 at a magnification of ×400. Red arrows highlight immune infiltrate.

negative impact on antigen-presenting cells as well as T lymphocytes,[31] suggesting that it could potentially impact the development of anti-tumor immunity. On the contrary, our findings using SAHA did not reveal an inhibition of either IFN responses in tumor cells or T cell ability to traffic to tumors. Moreover, enhanced IFN responses and robust T cell infiltration were observed following combinatorial therapy. An elevated macrophage infiltrate also suggests enhanced antigen presentation, but this has not yet been fully explored.

Reovirus individual therapy induces a robust immune response, with inflammatory cytokine production and the activation of both innate and adaptive immune responses in various tumor types.[13–19] This has also been corroborated in patients, wherein treatment with Reolysin resulted in the activation of both NK and cytotoxic T lymphocytes.[32] To determine the impact of this therapeutic strategy on mounting a successful anti-tumor immune response against HNSCCs, we utilized both immune-deficient and immune-competent murine tumor models. In female athymic nude mice lacking an intact T cell response, a significant increase in the survival of combination-treated mice was observed. IHC analysis of tumor sections from mice treated with SAHA and Reolysin also revealed a robust immune cell infiltrate, specifically macrophages, when compared to either agent alone. These data indicate that HDACi and reovirus treatment results in enhanced innate immune responses, even in the absence of adaptive immunity. Evaluation of the anti-tumor efficacy of this combination in a syngeneic mouse model of squamous carcinoma also revealed a significant macrophage and CD8 T cell tumor infiltration and enhancement of murine survival. This was accompanied by enhanced ex vivo anti-tumor "memory" responses, as elicited by a significant increase in tumor cell killing by splenocytes derived from animals treated with both agents. These data indicate a substantial therapeutic benefit following combination treatment for tumor-specific (most likely) T cell responses in both male and female mice. Taken together, combinatorial therapy enhanced both innate and adaptive immunity when compared to individual treatment groups.

Collectively our data demonstrate that treatment of Reolysin-infected animals with HDAC inhibitors increased both reovirus cytotoxic effects and anti-tumor immunity. Future studies will focus on

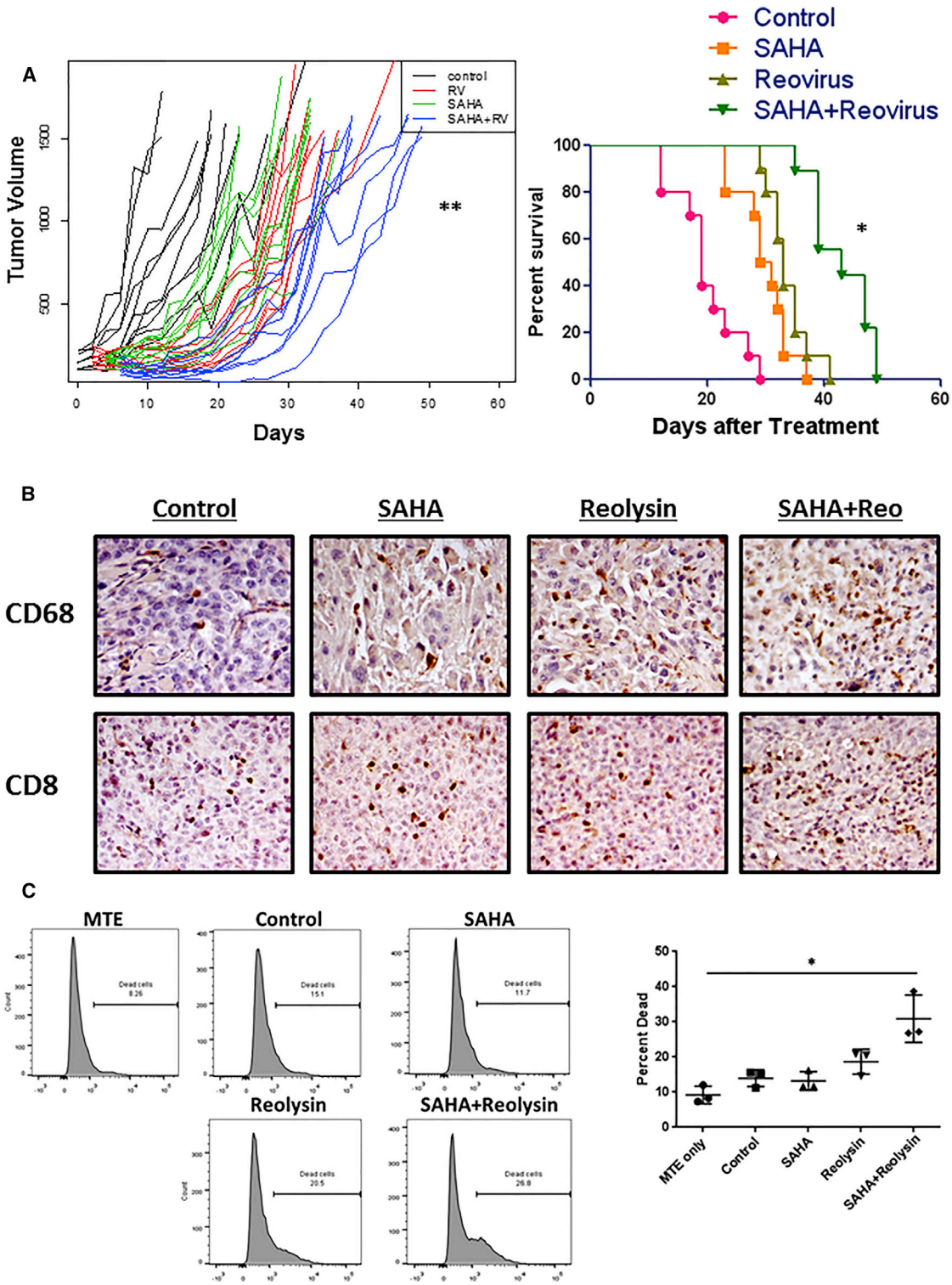

Figure 4. SAHA and Reolysin Combinatorial Therapy-Mediated Anti-Tumor Efficacy in a Murine Head and Neck Cancer Syngeneic Model

Immunocompetent C57BL/6 male mice (n = 10) bearing subcutaneous syngeneic MTE squamous tumors (treatment started at 150 mm^3) were treated with DMSO, SAHA (50 mg/kg via intraperitoneal injection on days 1, 3, 5, 8, and 10), Reolysin (Reo) (2.5×10^8 PFU via intratumoral injection on days 0, 3, and 10), or SAHA plus Reolysin combinatorial therapy. Mice were observed for tumor growth and euthanized when tumor burden reached removal criteria as per our Institutional Animal Care and Use

(legend continued on next page)

ascertaining the specific cell type(s) that are responsible for the therapeutic efficacy of combination therapy. Moreover, because murine studies were conducted in both male and female mice using a treatment schema that mirrors those used in patients, clinical studies may provide novel correlates to enhance ongoing and future clinical trials. This study provides the rationale for further investigation of this combination strategy in patients with HNSCCs.

MATERIALS AND METHODS

Cells, Reagents, and Viruses

Six human squamous cell carcinoma (SCC) cell lines (UM-SCC-74A, UM-SCC-1, UD-SCC-2, UM-SCC-11A, UM-SCC-47, and ATCC Cal27) as well as murine (MTE) squamous carcinoma cells (shPTP-BL-Ras) and murine fibroblasts (L929) were cultured as previously described.[33,34] All cells were propagated in DMEM (Life Technologies) supplemented with penicillin (100 U/mL), streptomycin (100 μg/mL), and 10% fetal bovine serum (FBS). Reolysin was kindly provided by Oncolytics Biotech. AR-42 was a gift from Arno Therapeutics and SAHA was purchased from Selleckchem.

Flow Cytometric Analysis

All flow cytometric analyses were conducting using a Becton Dickinson fluorescence-activated cell sorter (FACS) LSRII and analyzed using FloJo software as previously described.[9,35] JAM-1 surface levels were assessed using an anti-human or anti-mouse JAM-1 antibody (BD Biosciences Pharmingen) as compared to their respective isotype controls. The relative mean fluorescence intensity (MFI) was used to determine JAM-1 receptor surface levels. Cellular apoptosis was assessed using Annexin V-450 and propidium iodide staining (BD Biosciences Pharmingen) in accordance with the manufacturer's instructions. The percentage of dead cells was quantified using a Live/Dead Fixable Dead Cell Stain Kit (Invitrogen) per the manufacturer's instructions. The following antibodies were utilized for immune cell phenotypic analysis: CD49b-V450, F4/80-BV421, CD8-V450, CD44-PeCy7, CD62L-allophycocyanin (APC)-Cy7, CD11c-APC-Cy7, CD80-V450 (BD Biosciences Pharmingen), CD335-APC, CD11b-APC-Vio770, Gr1-APC, CD3-APC, CD4-fluorescein isothiocyanate (FITC), and major histocompatibility complex class II (MHCII)-FITC (Miltenyi Biotec).

WB Quantification and Immunostaining

WB using anti-σ-NS (reovirus capsid protein) and anti-JAM-1 (reovirus entry receptor) antibodies was performed as previously described.[8] WB results were quantified using ImageJ software (NIH). An anti-capsid protein antibody for immunostaining was kindly provided by Dr. Matt Coffey (Oncolytics Biotech) and used as previously described.[36] The avidin-biotin-peroxidase complex method was used for CD4, CD8, CD68, and NCR1 immunohistochemical detection. Briefly, 5-μm sections were cut from paraffin-embedded tumor specimens. After antigen retrieval in 0.01 M sodium citrate buffer (pH 6) at 100°C for 15 min, endogenous peroxidase was blocked by incubation with 3% hydrogen peroxide. The slides were incubated with donkey normal serum for 30 min at room temperature. The presence of antigens was evaluated using rabbit antibody at a dilution of 1:400. CD4 (bs-0647R), CD8 (bs-0648R), and NCR1 (bs-10027R) were purchased from Bioss, and CD68 (ab125212) was purchased from Abcam. After incubation with rabbit primary antibody, sections were incubated with the secondary biotinylated donkey anti-rabbit IgG (1:200; Jackson Laboratories) for 60 min at room temperature and then avidin-biotin-peroxidase complexes (VectaStain ABC Kit; Vector Laboratories) for 60 min. Reaction products were visualized with diaminobenzidine as the chromogen and sections were counterstained with Mayer's hematoxylin.

Real-Time PCR Analysis

To measure the changes in type I IFN pathway gene expression, RNA was purified using the RNeasy mini kit (QIAGEN). For real-time qPCR, cDNA was synthesized with the Superscript First-Strand Synthesis System (Invitrogen). Real-time continuous detection of PCR product was achieved using SYBR Green (Applied Biosystems). Glyceraldehyde 3-phosphate dehydrogenase (GAPDH) was used as an internal control. PCR primers are listed in Table 1 and were used as previously described.[20]

Viral Replication and Cell Viability Assays

L929 murine fibroblasts were utilized to determine reovirus replication using a standard PFU assay as previously described.[34] To assess head and neck carcinoma cell viability at various SAHA and AR-42 HDAC inhibitor concentrations and Reolysin MOIs, a standard 3-(4,5-dimethylthiazol-2-yl)-2,5-diphenyltetrazolium bromide (MTT) assay was performed following 48 hr of treatment, as previously described.[37] Half maximal inhibitory concentration (IC_{50}) values were interpolated from a sigmoidal dose-response curve fit of the log-transformed survival data.

Animal Studies

All murine studies were performed in accordance with the Institutional Review Board and the Subcommittee on Research Animal Care at The Ohio State University. Female athymic nu/nu (Target Validation Shared Resource, The Ohio State University) or C57BL/6

Committee (IACUC) protocol. (A) Tumor volume growth was assessed over time for each mouse in every treatment group. **$p < 0.0001$ (difference between combination-treated mice and all other treatment groups; left panel). Kaplan-Meir plots of mice bearing subcutaneous MTE tumors treated with SAHA, reovirus, or the combination as indicated (the treatment schema is indicated below the plot). *$p < 0.01$ (combination treatment differences compared to each individual treatment group). All survival studies were performed in duplicate. (B) Representative macrophage- (CD68) and T cell (CD8)-stained tumors at time of death when tumors reached ~1,500 mm^3 at a magnification of ×400. (C) In a separate experiment, splenocytes from mice treated with reovirus, HDACis, or both were cultured with tumor cells and tumor cell killing was evaluated by live and dead cell staining. Data shown are representative histograms from the flow cytometric analysis of day 7 splenocytes following 48-hr ex vivo co-culture with MTE tumor cells at a ratio of 4:1, respectively. The right panel is the quantification of killing (n = 3 mice/group). *$p < 0.01$ (combination treatment differences compared to each individual treatment group). Murine studies were performed in duplicate.

Table 1. Primer List for Gene Expression Analysis in Human SCC74A and MTE Cell Lines

Cell Line	Gene	Sequence
SCC74A	human IFNα sense	5′-AGCCATCTCTGTCCTCCATGAG-3′
	human IFNα anti-sense	5′-TGCATCACACAGGCTTCCAA-3′
	human MCP1 sense	5′-ATCTCCTTGGCCACAATGGTC-3′
	human MCP1 anti-sense	5′-AGATGCAATCAATGCCCCAG-3′
	human GAPDH sense	5′-GGAGTCAACGGATTTGGTCG-3′
	human GAPDH anti-sense	5′-GGAATCATATTGGAACATGTA AACC-3′
MTE	murine IFNα sense	5′-CCTGCTGGCTGTGAGGAAATA-3′
	murine IFNα anti-sense	5′-TCTCAGTCTTCCCAGCACATTG-3′
	murine MCP1 sense	5′-AACCTGGATCGGAACCAAATG-3′
	murine MCP1 anti-sense	5′-GCTTGAGGTGGTTGTGGAAAAG-3′
	murine GAPDH sense	5′-AGCCTCGTCCCGTAGACAAAAT-3′
	murine GAPDH anti-sense	5′-GAAGACACCAGTAGACTCCACG ACAT-3′

Primer list for real-time continuous detection of PCR products using SYBR Green. GAPDH was used as an internal control. IFN, interferon; GAPDH, glyceraldehyde 3-phosphate dehydrogenase; MCP, monocyte chemotactic protein.

male mice (Jackson Laboratories), aged 4–5-weeks, were injected subcutaneously with SCC-74A (1.5×10^7) or MTE (murine syngeneic) (1×10^6) cells in a volume of 100 μL into the rear flank, respectively. Mice were then recruited into studies and randomized into treatment groups as previously described.[33] For SCC-74A (human xenograft) studies, mice were treated with 2×10^9 PFU Reolysin on days 0 and 7 post-recruitment and SAHA (50 mg/kg) was administered via intraperitoneal (i.p.) injection 5 days per week for the duration of the study. For MTE studies, mice were treated with 2.5×10^8 PFU on days 0, 3, and 10 post-recruitment and SAHA (50 mg/kg) was administered via i.p. injection on days 1, 3, 5, 8, 10, and 12. Tissues were harvested at the indicated time points for ex vivo killing[38] or immune cell phenotypic assessment and for tumor H&E immunohistochemistry (when tumors reached ~1,500 mm^3)[33] as described. Animals were observed daily and tumor volumes were obtained as previously described.[33] Mice were euthanized when the tumor burden reached ~1,500 mm^3, if there was a >20% body mass loss, or at the indicated time points according to animal care and usage guidelines. All animal experiments were performed in duplicate.

Statistical Analysis

GraphPad Prism 6 (GraphPad Software), R3.3.1 (R Foundation for Statistical Computing), and SAS 9.3 (SAS Institute) were used for statistical analysis. A one-way ANOVA model was used to compare three or more conditions, such as JAM-1 expression and reovirus titer. A two-way ANOVA model and a Chou-Talalay analysis were used for interaction contrasts or synergistic effect tests. For the Chou-Talalay analysis, data are presented as the fraction affected versus CI plots. CI < 1, CI = 1, and CI > 1 indicate synergistic, additive, and antagonistic interactions, respectively, using CompuSyn software (Biosoft). Tumor volume comparisons between each treatment group were assessed using a linear mixed model to account for repeated measures over time for each mouse. Group means and tumor growth rate over time were compared between any two of groups and p values were adjusted for multiple comparisons using the Holm's procedure. For survival data, survival functions were estimated by the Kaplan-Meier method and were compared with the log-rank test among the groups. The p value was adjusted for multiple comparisons by Holm's procedure. A p value of 0.05 or less was considered statistically significant.

SUPPLEMENTAL INFORMATION

Supplemental Information includes three figures and can be found with this article online at http://dx.doi.org/10.1016/j.omto.2017.05.002.

AUTHOR CONTRIBUTIONS

A.C.J.-R. and J.-G.Y. designed and conducted experiments and wrote the paper. E.C., J.Y.Y., and T.J.L. designed and conducted experiments. J.Z. conducted the formal statistical analyses. C.H., J.H.L., B.K., Q.P., P.K., R.B., T.T., and F.P. assisted in project design and manuscript preparation and editing. B.K. and M.O. conceptualized and designed experiments, supervised, provided funding support, and wrote the paper.

CONFLICTS OF INTEREST

No potential conflicts of interest were disclosed.

ACKNOWLEDGMENTS

We acknowledge the Analytical Cytometry Shared Resource, the Center for Biostatistics, and the Target Validation Shared Resources within the James Comprehensive Cancer Center, all at The Ohio State University. This work was supported by NIH grants R01-NS064607, P01-CA163205, R01-CA150153, and P30-CA016058 (to B.K.), NIH grant F32CA186542, an Ohio State University Comprehensive Cancer Center Pelotonia Postdoctoral Candidate Fellowship (to A.C.J.-R.), and an Ohio State University Comprehensive Cancer Center Joan Bisesi Memorial Career Development Grant.

REFERENCES

1. Meisen, W.H., and Kaur, B. (2013). How can we trick the immune system into overcoming the detrimental effects of oncolytic viral therapy to treat glioblastoma? Expert Rev. Neurother. *13*, 341–343.
2. Pol, J., Kroemer, G., and Galluzzi, L. (2015). First oncolytic virus approved for melanoma immunotherapy. OncoImmunology *5*, e1115641.
3. Black, A.J., and Morris, D.G. (2012). Clinical trials involving the oncolytic virus, reovirus: ready for prime time? Expert Rev. Clin. Pharmacol. *5*, 517–520.
4. Ferreira, M.B., Lima, J.P., and Cohen, E.E. (2012). Novel targeted therapies in head and neck cancer. Expert Opin. Investig. Drugs *21*, 281–295.
5. West, A.C., and Johnstone, R.W. (2014). New and emerging HDAC inhibitors for cancer treatment. J. Clin. Invest. *124*, 30–39.
6. Mann, B.S., Johnson, J.R., Cohen, M.H., Justice, R., and Pazdur, R. (2007). FDA approval summary: vorinostat for treatment of advanced primary cutaneous T-cell lymphoma. Oncologist *12*, 1247–1252.
7. Nervi, C., De Marinis, E., and Codacci-Pisanelli, G. (2015). Epigenetic treatment of solid tumours: a review of clinical trials. Clin. Epigenetics *7*, 127.

8. Stiff, A., Caserta, E., Sborov, D.W., Nuovo, G.J., Mo, X., Schlotter, S.Y., Canella, A., Smith, E., Badway, J., Old, M., et al. (2016). Histone deacetylase inhibitors enhance the therapeutic potential of reovirus in multiple myeloma. Mol. Cancer Ther. *15*, 830–841.

9. Yoo, J.Y., Jaime-Ramirez, A.C., Bolyard, C., Dai, H., Nallanagulagari, T., Wojton, J., Hurwitz, B.S., Relation, T., Lee, T.J., Lotze, M.T., et al. (2016). Bortezomib treatment sensitizes oncolytic HSV-1-treated tumors to NK cell immunotherapy. Clin. Cancer Res. *22*, 5265–5276.

10. Chang, H.M., Paulson, M., Holko, M., Rice, C.M., Williams, B.R., Marié, I., and Levy, D.E. (2004). Induction of interferon-stimulated gene expression and antiviral responses require protein deacetylase activity. Proc. Natl. Acad. Sci. USA *101*, 9578–9583.

11. Marchini, A., Scott, E.M., and Rommelaere, J. (2016). Overcoming barriers in oncolytic virotherapy with HDAC inhibitors and immune checkpoint blockade. Viruses *8*, E9.

12. Nusinzon, I., and Horvath, C.M. (2003). Interferon-stimulated transcription and innate antiviral immunity require deacetylase activity and histone deacetylase 1. Proc. Natl. Acad. Sci. USA *100*, 14742–14747.

13. Errington, F., Steele, L., Prestwich, R., Harrington, K.J., Pandha, H.S., Vidal, L., de Bono, J., Selby, P., Coffey, M., Vile, R., and Melcher, A. (2008). Reovirus activates human dendritic cells to promote innate antitumor immunity. J. Immunol. *180*, 6018–6026.

14. Errington, F., White, C.L., Twigger, K.R., Rose, A., Scott, K., Steele, L., Ilett, L.J., Prestwich, R., Pandha, H.S., Coffey, M., et al. (2008). Inflammatory tumour cell killing by oncolytic reovirus for the treatment of melanoma. Gene Ther. *15*, 1257–1270.

15. Gujar, S.A., Marcato, P., Pan, D., and Lee, P.W. (2010). Reovirus virotherapy overrides tumor antigen presentation evasion and promotes protective antitumor immunity. Mol. Cancer Ther. *9*, 2924–2933.

16. Gujar, S.A., Pan, D.A., Marcato, P., Garant, K.A., and Lee, P.W. (2011). Oncolytic virus-initiated protective immunity against prostate cancer. Mol. Ther. *19*, 797–804.

17. Hall, K., Scott, K.J., Rose, A., Desborough, M., Harrington, K., Pandha, H., Parrish, C., Vile, R., Coffey, M., Bowen, D., et al. (2012). Reovirus-mediated cytotoxicity and enhancement of innate immune responses against acute myeloid leukemia. Biores. Open Access *1*, 3–15.

18. Prestwich, R.J., Errington, F., Ilett, E.J., Morgan, R.S., Scott, K.J., Kottke, T., Thompson, J., Morrison, E.E., Harrington, K.J., Pandha, H.S., et al. (2008). Tumor infection by oncolytic reovirus primes adaptive antitumor immunity. Clin. Cancer Res. *14*, 7358–7366.

19. Prestwich, R.J., Ilett, E.J., Errington, F., Diaz, R.M., Steele, L.P., Kottke, T., Thompson, J., Galivo, F., Harrington, K.J., Pandha, H.S., et al. (2009). Immune-mediated antitumor activity of reovirus is required for therapy and is independent of direct viral oncolysis and replication. Clin. Cancer Res. *15*, 4374–4381.

20. Otsuki, A., Patel, A., Kasai, K., Suzuki, M., Kurozumi, K., Chiocca, E.A., and Saeki, Y. (2008). Histone deacetylase inhibitors augment antitumor efficacy of herpes-based oncolytic viruses. Mol. Ther. *16*, 1546–1555.

21. Comins, C., Spicer, J., Protheroe, A., Roulstone, V., Twigger, K., White, C.M., Vile, R., Melcher, A., Coffey, M.C., Mettinger, K.L., et al. (2010). REO-10: a phase I study of intravenous reovirus and docetaxel in patients with advanced cancer. Clin. Cancer Res. *16*, 5564–5572.

22. Galanis, E., Markovic, S.N., Suman, V.J., Nuovo, G.J., Vile, R.G., Kottke, T.J., Nevala, W.K., Thompson, M.A., Lewis, J.E., Rumilla, K.M., et al. (2012). Phase II trial of intravenous administration of Reolysin(R) (reovirus serotype-3-Dearing strain) in patients with metastatic melanoma. Mol. Ther. *20*, 1998–2003.

23. Hingorani, P., Zhang, W., Lin, J., Liu, L., Guha, C., and Kolb, E.A. (2011). Systemic administration of reovirus (Reolysin) inhibits growth of human sarcoma xenografts. Cancer *117*, 1764–1774.

24. Morris, D.G., Feng, X., DiFrancesco, L.M., Fonseca, K., Forsyth, P.A., Paterson, A.H., Coffey, M.C., and Thompson, B. (2013). REO-001: a phase I trial of percutaneous intralesional administration of reovirus type 3 dearing (Reolysin®) in patients with advanced solid tumors. Invest. New Drugs *31*, 696–706.

25. Green, D.R., Ferguson, T., Zitvogel, L., and Kroemer, G. (2009). Immunogenic and tolerogenic cell death. Nat. Rev. Immunol. *9*, 353–363.

26. Hanahan, D., and Weinberg, R.A. (2011). Hallmarks of cancer: the next generation. Cell *144*, 646–674.

27. Ichim, G., and Tait, S.W. (2016). A fate worse than death: apoptosis as an oncogenic process. Nat. Rev. Cancer *16*, 539–548.

28. Christiansen, A.J., West, A., Banks, K.M., Haynes, N.M., Teng, M.W., Smyth, M.J., and Johnstone, R.W. (2011). Eradication of solid tumors using histone deacetylase inhibitors combined with immune-stimulating antibodies. Proc. Natl. Acad. Sci. USA *108*, 4141–4146.

29. Setiadi, A.F., Omilusik, K., David, M.D., Seipp, R.P., Hartikainen, J., Gopaul, R., Choi, K.B., and Jefferies, W.A. (2008). Epigenetic enhancement of antigen processing and presentation promotes immune recognition of tumors. Cancer Res. *68*, 9601–9607.

30. Alvarez-Breckenridge, C.A., Yu, J., Price, R., Wei, M., Wang, Y., Nowicki, M.O., Ha, Y.P., Bergin, S., Hwang, C., Fernandez, S.A., et al. (2012). The histone deacetylase inhibitor valproic acid lessens NK cell action against oncolytic virus-infected glioblastoma cells by inhibition of STAT5/T-BET signaling and generation of gamma interferon. J. Virol. *86*, 4566–4577.

31. Akimova, T., Beier, U.H., Liu, Y., Wang, L., and Hancock, W.W. (2012). Histone/protein deacetylases and T-cell immune responses. Blood *119*, 2443–2451.

32. White, C.L., Twigger, K.R., Vidal, L., De Bono, J.S., Coffey, M., Heinemann, L., Morgan, R., Merrick, A., Errington, F., Vile, R.G., et al. (2008). Characterization of the adaptive and innate immune response to intravenous oncolytic reovirus (Dearing type 3) during a phase I clinical trial. Gene Ther. *15*, 911–920.

33. Yoo, J.Y., Yu, J.G., Kaka, A., Pan, Q., Kumar, P., Kumar, B., Zhang, J., Mazar, A., Teknos, T.N., Kaur, B., and Old, M.O. (2015). ATN-224 enhances antitumor efficacy of oncolytic herpes virus against both local and metastatic head and neck squamous cell carcinoma. Mol Ther Oncolytics *2*, 15008.

34. Twigger, K., Vidal, L., White, C.L., De Bono, J.S., Bhide, S., Coffey, M., Thompson, B., Vile, R.G., Heinemann, L., Pandha, H.S., et al. (2008). Enhanced in vitro and in vivo cytotoxicity of combined reovirus and radiotherapy. Clin. Cancer Res. *14*, 912–923.

35. Bolyard, C., Meisen, W.H., Banasavadi-Siddegowda, Y., Hardcastle, J., Yoo, J.Y., Wohleb, E.S., Wojton, J., Yu, J.G., Dubin, S., Khosla, M., et al. (2017). BAI1 orchestrates macrophage inflammatory response to HSV infection–implications for oncolytic viral therapy. Clin. Cancer Res. *23*, 1809–1819.

36. Sborov, D.W., Nuovo, G.J., Stiff, A., Mace, T., Lesinski, G.B., Benson, D.M., Jr., Efebera, Y.A., Rosko, A.E., Pichiorri, F., Grever, M.R., and Hofmeister, C.C. (2014). A phase I trial of single-agent Reolysin in patients with relapsed multiple myeloma. Clin. Cancer Res. *20*, 5946–5955.

37. Yoo, J.Y., Hurwitz, B.S., Bolyard, C., Yu, J.G., Zhang, J., Selvendiran, K., Rath, K.S., He, S., Bailey, Z., Eaves, D., et al. (2014). Bortezomib-induced unfolded protein response increases oncolytic HSV-1 replication resulting in synergistic antitumor effects. Clin. Cancer Res. *20*, 3787–3798.

38. Jaime-Ramirez, A.C., Mundy-Bosse, B.L., Kondadasula, S., Jones, N.B., Roda, J.M., Mani, A., Parihar, R., Karpa, V., Papenfuss, T.L., LaPerle, K.M., et al. (2011). IL-12 enhances the antitumor actions of trastuzumab via NK cell IFN-γ production. J. Immunol. *186*, 3401–3409.